Single attosecond pulse generation with intense mid-infrared elliptically polarized laser pulses

F. He,[1,*] C. Ruiz,[1] and A. Becker[1]

[1]*Max-Planck-Institut für Physik Komplexer Systeme, Nöthnitzer Strasse 38, D-01187 Dresden, Germany*
Corresponding author: fhe@pks.mpg.de

Received May 18, 2007; revised September 10, 2007; accepted September 25, 2007; posted September 26, 2007 (Doc. ID 83225); published October 31, 2007

We have studied theoretically high-harmonic-order and single attosecond pulse generation with elliptically polarized laser pulses at wavelengths ranging from the visible to the mid-infrared. Results of *ab initio* simulations of the time-dependent Schrödinger equation show that the ellipticity dependence of the high-harmonic signal intensifies with increasing wavelength of the driving pulse and saturates in the mid-infrared. The isolation of single attosecond pulses using the polarization gating method in the mid-infrared is due to an effective suppression of side pulses as compared with an operation at Ti:sapphire wavelengths.

OCIS codes: 190.4160, 190.2620, 190.7110, 190.4180, 020.4180.

One of the major achievements in laser technology in recent years has been the generation of intense pulses at XUV wavelengths with attosecond duration [1–5]. Attosecond pulses are produced by high-harmonic generation (HHG) from a driving laser pulse at high intensity. According to the three-step picture [6,7] HHG can be understood as the ionization of an electron by tunneling followed by the acceleration of the electron in the field. In the case of linear polarization of the field the electron can return to and recombine with the parent ion. The last step is accompanied by the emission of a harmonic photon. In an oscillating field this process repeats every half-cycle, which leads in a multicycle driving pulse to a train of attosecond pulses [2]. Isolated single attosecond pulses have been realized using two approaches: by the selection of high-energy cutoff harmonics from a few-cycle fundamental pulse [1,4] or by using a polarization gating technique [5,8–10].

The polarization gating method is based on the strong dependence of the generation of high harmonics on the ellipticity of the driving pulse. The transverse field component causes the ionized electron wave packet to be driven away from the parent ion. Consequently the the high-harmonic signal falls off rapidly with increasing ellipticity. This feature of HHG has been used by modulating the driving laser pulse such that it is only linearly polarized during its central part while elliptically polarized elsewhere [5,10].

Nowadays, studies on strong-field processes usually focus on the near-infrared wavelength regime. However, HHG should depend on the wavelength λ of the fundamental pulse, since the quiver radius $\alpha_0 \sim \lambda^2$ and the ponderomotive energy $U_p \sim \lambda^2$. Due to the cutoff of HHG at $3.17U_p+I_p$, where I_p is the ionization potential of the atom, longer driving wavelengths will generate higher-order harmonics [11]. But the efficiency of the harmonic yields drops due to the larger quiver radius and hence the larger spreading of the wavepacket. One should further expect that the ellipticity dependence intensifies when the quiver radius increases. Thus, it may be useful to generate single attosecond pulses via the polarization gating technique from fundamental pulses at mid-infrared or infrared wavelengths.

In this Letter we compare the ellipticity dependence of HHG and the generation of single attosecond pulses using the polarization gating method at conventional near-infrared with those at mid-infrared wavelengths theoretically. To this end, we have analyzed the single-atom response by performing *ab initio* simulations of the time-dependent Schrödinger equation of the hydrogen atom interacting with an elliptically polarized intense laser pulse. For the calculations we have used the three-dimensional model for the hydrogen atom given in dipole approximation and length gauge by (Hartree atomic units, $e=m=\hbar=1$ are used):

$$i\frac{\partial}{\partial t}\Phi(\mathbf{r};t)=[H_0+\mathbf{E}(t)\cdot\mathbf{r}]\Phi(\mathbf{r};t), \tag{1}$$

where $\mathbf{E}(t)$ is the electric field and

$$H_0=-\frac{1}{2}\nabla_{\mathbf{r}}^2-\frac{1}{\sqrt{\mathbf{r}^2+\alpha}} \tag{2}$$

is the field-free Hamiltonian. We have chosen the soft core parameter $\alpha=0.115$ such that the model yields the experimental ground state energy of −0.5 a.u. The wave function has been propagated on a grid using the Crank–Nicholson method with grid parameters $\Delta x=\Delta y=\Delta z=0.3$ a.u., and the time step was $\Delta t=0.1$ a.u. The number of grid points varied with the wavelength and extended up to $N_x=700$, $N_y=500$, and $N_z=50$ for the longest wavelengths considered. We have used the exterior complex scaling method to suppress reflections from the edges of the numerical grid (e.g., [12]). The ground state was obtained using imaginary time propagation.

We first investigate the ellipticity dependence of the HHG spectrum at different laser wavelengths. To

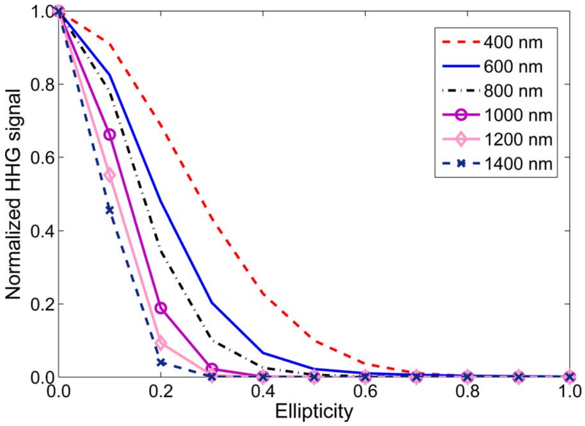

Fig. 1. (Color online) HHG signal, integrated over all harmonic orders with $\Omega > 2U_p + I_p$ as a function of ellipticity for different laser wavelengths (see legend). The signals are normalized to the result obtained in the case of linear polarization at a given wavelength.

this end, we have considered an elliptically polarized pulse with a temporal Gaussian shape described by

$$\mathbf{E}(t) = E_0(t)(E_x(t)\hat{x} + E_y(t)\hat{y}), \quad (3)$$

with $E_0(t) = E_0 \exp[-8 \ln 2(t/\tau)^2]$ as the slowly varying envelope and the two components defined as

$$E_x(t) = \frac{1}{\sqrt{1+\epsilon^2}} \cos(\omega t), \quad (4)$$

$$E_y(t) = \frac{\epsilon}{\sqrt{1+\epsilon^2}} \sin(\omega t), \quad (5)$$

where E_0, ϵ, and ω are the amplitude, ellipticity, and frequency of the field, respectively, and τ is the pulse duration. The field is linearly (circularly) polarized as $\epsilon=0$ ($\epsilon=1$).

The high-harmonic spectra have been obtained by evaluating the second derivative of the time-dependent dipole moment, expanding it in a Fourier series $f(\Omega)$, and taking the coherent response $|f(\Omega)|^2$. In Fig. 1 we present the results for the harmonic signal, integrated over all harmonic orders with $\Omega > 2U_p + I_p$, with $U_p = I_0/4\omega^2$ as a function of the ellipticity for different wavelengths ranging from 400 to 1400 nm (see legend). E_0 is fixed to 0.05 a.u., corresponding to a laser intensity of $I_0 = 8.8 \times 10^{13}$ W/cm^2, and $\tau = 6T$, where T is the oscillation period of the field, in all calculations. For comparison the signals are normalized to the result obtained in the case of linear polarization at a given wavelength. The signals show the expected rapid drop with increasing ellipticity. The ellipticity dependence intensifies as the wavelength sweeps from the visible to the mid-infrared and appears to saturate at about 1400 nm. The signal drops to half the value obtained for a linearly polarized field for $\epsilon_{1/2} = 0.28$, 0.17, and 0.09 for $\lambda = 400$, 800, and 1400 nm, respectively.

Thus, generation of single attosecond pulses via the polarization gating technique using mid-infrared driving pulses should be indeed useful. To test our expectation we have performed another set of calculations for an ellipticity modulated electric field with the two fields components given by [9]

$$E_x(t) = \frac{1}{2}(E_0^+(t) - E_0^-(t))\cos(\omega t), \quad (6)$$

$$E_y(t) = \frac{1}{2}(E_0^+(t) + E_0^-(t))\sin(\omega t), \quad (7)$$

with $E_0^{\pm}(t) = E_0(t \pm \delta/2)$, where δ is the delay introduced by the polarization gate between E_0^+ and E_0^-.

We have considered ellipticity modulated pulses in the near-infrared ($\lambda = 800$ nm) and in the mid-infrared ($\lambda = 1400$ nm) with $E_0 = 0.092$ a.u., corresponding to the laser intensity $I_0 = 3 \times 10^{14}$ W/cm^2, $\tau = 8T$, and $\delta = 5T$. The maximum amplitude in the modulated pulse is 0.0544 a.u. In Figs. 2(a) the two field components, $E_x(t)$ and $E_y(t)$, and 2(b) the ellipticity are shown as a function of time scaled in units of T. In this representation the variation of the field components is independent of the wavelength, which enables us to compare the attosecond pulse generation from driving pulses with the same number of cycles but at different frequencies.

In Fig. 3 we present a time–frequency analysis of the harmonic response at 800 nm (upper panel) and 1400 nm (lower panel). It has been obtained using the short-time Fourier (or wavelet) transform with a frequency window that covers the whole harmonic spectrum (except the fundamental) [13]. While for the near-infrared laser pulses there are several bursts at high-harmonic energies, in the mid-infrared just one significant burst occurs. This is due to the smaller half-width $\epsilon_{1/2}$ in the latter case, which restricts the effective HHG to one cycle at the center of the pulse [see Fig. 2(b)]. Consequently, just a single attosecond laser pulse is generated using the mid-infrared fundamental [Fig. 4(b)], while at $\lambda = 800$ nm a train of three pulses is seen [Fig. 4(a)]. The pulses

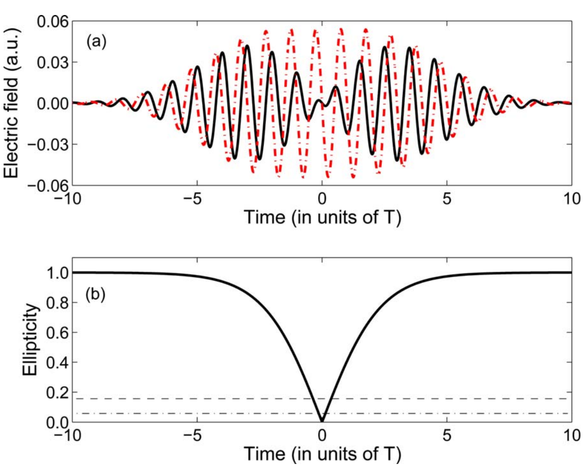

Fig. 2. (Color online) (a) Electric field components E_x (solid line) and E_y (dashed line) and (b) ellipticity as a function of time. The two lines in panel (b) represent $\epsilon_{1/2}$ at 800 nm (dashed–dotted line) and 1400 nm (dashed–dotted) line.

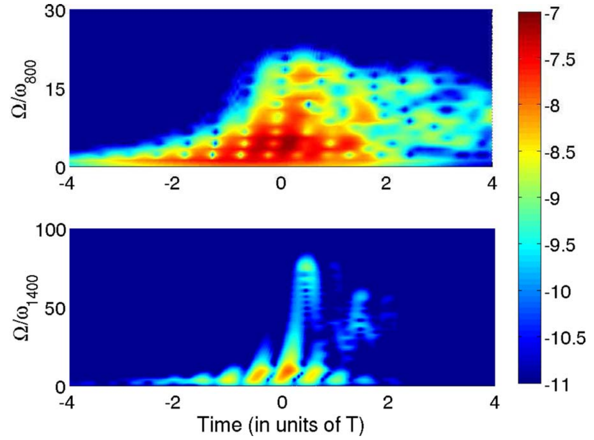

Fig. 3. (Color online) Time–frequency analysis (on a logarithmic scale) using a wavelet transform for fundamental laser pulses operating at 800 nm (upper panel) and 1400 nm (lower panel). Parameters are as in Fig. 2.

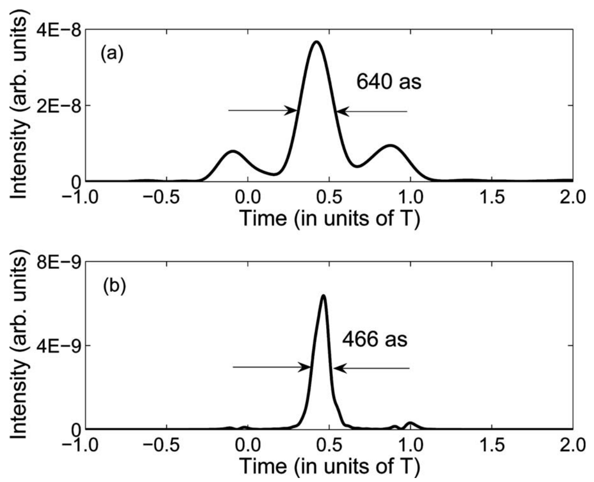

Fig. 4. Attosecond laser pulses generated from the harmonics with $\Omega > 0.8\omega_{cutoff}$ from (a) 800 nm and (b) 1400 nm driving pulses. Parameters are as in Fig. 2.

are obtained by integrating the intensity of all harmonics with $\Omega > 0.8\omega_{cutoff}$, where ω_{cutoff} is the cutoff frequency of the high-harmonic spectrum, which is 1.22 and 2.7 a.u. for 800 and 1400 nm, respectively. The central photon energies are 1 and 2.6 a.u. in Fig. 4(a) and 4(b), respectively. The pulse duration (without compensation of the harmonic phases) is shorter in the mid-infrared case. However, the intensity generated from the mid-infrared pulse is reduced by about a factor of 5 compared with the generation at 800 nm.

HHG depends on both the singe-atom response and the propagation of the generated pulse in the ionizing medium. Solution of the full problem would require the simulation of a combined approach based on the time-dependent Schrödinger equation and the Maxwell equations over a macroscopic region, which is beyond the limit of current computer resources. In general, phase matching becomes more difficult at longer wavelengths due to the decrease of the coherence length. However, recent theoretical analyses [14,15] have revealed conditions for nonadiabatic self-phase matching that may increase the conversion efficiency by orders of magnitude at mid-infrared wavelengths [15]. Furthermore, there have been reported techniques of active phase correction [16,17].

To summarize, we have studied the generation of single attosecond laser pulses with driving pulses modulated by a polarization gate. It is found that the ellipticity dependence of the high-harmonic signal intensifies with increasing wavelength of the fundamental, but saturates in the mid-infrared. Consequently, longer pulses with more cycles can be used in the mid-infrared compared with the near-infrared to obtain a single attosecond pulse.

We acknowledge contributions by S. Baier, P. Panek, and A. Requate to the virtual laser lab Nonlinear Processes in Strong Fields Library, which has been used for the present calculations.

References

1. M. Hentschel, R. Kienberger, Ch. Spielmann, G. A. Reider, N. Milosevic, T. Brabec, P. Corkum, U. Heinzmann, M. Drescher, and F. Krausz, Nature **414**, 509 (2001).
2. P. M. Paul, E. S. Toma, P. Breger, G. Mullot, F. Augé, P. Balcou, H. G. Muller, and P. Agostini, Science **292**, 1689 (2001).
3. P. Tzallas, D. Charalambidis, N. A. Papadogiannis, K. Witte, and G. D. Tsakiris, Nature **426**, 267 (2003).
4. R. Kienberger, E. Goulielmakis, M. Uiberacker, A. Baltuska, V. Yakovlev, F. Bammer, A. Scrinzi, Th. Westerwalbesloh, U. Kleineberg, U. Heinzmann, M. Drescher, and F. Krausz, Nature **427**, 817 (2004).
5. G. Sansone, E. Benedetti, F. Calegari, C. Vozzi, L. Avaldi, R. Flammini, L. Poletto, P. Villoresi, C. Altucci, R. Velotta, S. Stagira, S. De Silvestri, and M. Nisoli, Science **314**, 443 (2006).
6. J. F. Krause, K. J. Schafer, and K. C. Kulander, Phys. Rev. Lett. **68**, 3535 (1992).
7. P. B. Corkum, Phys. Rev. Lett. **71**, 1994 (1993).
8. P. B. Corkum, N. H. Burnett, and M. Yu. Ivanov, Opt. Lett. **19**, 1870 (1994).
9. V. Strelkov, A. Zair, O. Tcherbakoff, R. López-Martens, E. Cormier, E. Mével, and E. Constant, Appl. Phys. B: Photophys. Laser Chem. **78**, 879 (2004).
10. I. J. Sola, E. Mével, L. Elouga, E. Constant, V. Strelkov, L. Poletto, P. Villoresi, E. Benedetti, J.-P. Caumes, S. Stagira, C. Vozzi, G. Sansone, and M. Nisoli, Nature **2**, 319 (2006).
11. J. Tate, T. Auguste, H. G. Muller, P. Salières, P. Agostini, and L. F. DiMauro, Phys. Rev. Lett. **98**, 013901 (2007).
12. F. He, C. Ruiz, and A. Becker, Phys. Rev. A **75**, 053407 (2007).
13. P. Lan, P. Lu, W. Cao, X. Wang, and G. Yang, Phys. Rev. A **74**, 063411 (2006).
14. M. Geissler, G. Tempea, and T. Brabec, Phys. Rev. A **62**, 033817 (2000).
15. V. S. Yakovlev, M. Ivanov, and F. Krausz, "Enhanced phase-matching for generation of soft-X-ray harmonics and attosecond pulses in atomic gases," Opt. Express (to be published).
16. X. Zhang, A. L. Lytle, T. Popmintchev, X. Zhou, H. C. Kapteyn, M. M. Murnane, and O. Cohen, Nat. Phys. **3**, 270 (2007).
17. C. A. Haworth, L. E. Chipperfield, J. S. Robinson, P. L. Knight, J. P. Marangos, and J. W. G. Tisch, Nat. Phys. **3**, 52 (2007).